VARIABLE TEMPERATURE HOT WIRE ANEMOMETRY APPLIED TO THE JOINT ANALYSIS OF THE VELOCITY AND TEMPERATURE FLUCTUATIONS IN A MIXING LAYER

Malick Ndoye[1,2,3], **Joel Delville**[2], **Eva Dorignac**[2], **Georges Arroyo**[1,3]

[1]Cemagref - UR TERE
17 avenue de Cucillé, F-35044 Rennes, France
malick.ndoye@cemagref.fr, georges.arroyo@cemagref.fr

[2]Department Fluide Thermique Combustion
Institut PPRIME/ CNRS - Université de Poitiers - ENSMA UPR 3346
CEAT, 43 rue de l'Aérodrome, F-86036 Poitiers cedex, France
malick.ndoye@lea.univ-poitiers.fr, joel.delville@univ-poitiers.fr, eva.dorignac@univ-poitiers.fr

[3]Université Européenne de Bretagne
France

1 Abstract

Our study provides a detailed description of the thermal mixing process in an anisothermal mixing layer. Velocity and temperature are simultaneously measured at the same point by using a new hot wire anemometer. This anemometer implements the multiple overheat principle, associated with a non linear Levenberg-Marquardt signal processing. These simultaneous measurements allowed an analysis based on conditional Probability Density Functions (PDFs), joint PDFs and a quadrant analysis. Variable temperature hot wire anemometry clearly proved its ability to give access, in particular, to a precise description of the contributions of saddle point ejections to the thermal turbulent mixing process.

2 Introduction

Anisothermal mixing layers (Fiedler (1974)) are present in many industrial applications and environmental flows, particularly when localized thermal environment separations are involved. In this case, the improvement of the thermal confinement by mixing reduction in situations of mixing layer type requires the understanding of the inherent relations between the mechanical stirring imposed by the velocity field and the temperature fluctuations. This coupling is present in the scalar transport equations in terms of a vectorial heat flux, one component of which is $\overline{u'T'}$.

Most of the past studies on scalar mixing layers (temperature, concentration and / or density) emphasized the differences between dynamic and scalar behaviors. Faster and greater development is generally observed in the dynamic field compared to the scalar field. In his study of a heated plane mixing layer with a zero velocity ratio, Fiedler (1974) observed dissymmetrical average and RMS temperature profiles, with a triple inflexion point and a bi-modal shape, respectively, thus clearly different from those of the velocity field. Similar results were also obtained in gaseous mixing layer studies by Brown & Roshko (1974), Batt (1977) and Masutani & Bowman (1986), and, more recently, in simulations of heat transfer by Bisset (1997). Probability density functions (PDF) are commonly used to describe the scalar mixing process. Two categories of scalar PDF can generally be obtained in the mixing layer, the marching type or the non-marching type, as denoted among others by Bisset (1997) and Pickett & Ghandi (2001, 2002) in their Planar Laser Induced Velocimetry scalar measurement in an incompressible mixing layer. Marching means here that the shape of the PDF continuously evolves as the measurement point is moved across the mixing layer. Karasso & Mungal (1996) stated that the final stage of a high Reynolds mixing layer is characterized by marching type PDFs of the scalar.

Our study provides a detailed description of the mixing process in a plane anisothermal mixing layer, by the analysis of the correlations between velocity and temperature fluctuations. The flow configuration studied, with a cold rapid layer above a hot slow one, corresponds to industrial and atmospheric situations that motivated this work (separation of a lower cold layer from a warm atmosphere). The data were obtained with a new variable temperature hot wire anemometer relying on a parameterizable variation of the overheat ratio of a single hot wire. A specific signal processing was developed in association with this multiple overheat principle. Such an anemometer enables quasi-simultaneous measurements of the local velocity and temperature at the same point. The synchronism of the measurements then allows a fine analysis of

the relationships between the fluctuations of the two physical quantities considered in the mixing process. These relationships were analyzed using a joint probability density function approach and a quadrant decomposition method which consists in splitting the heat flux into four quadrants, classically defined as the four possible contributions of the instantaneous values of the fluctuations $u'(t)$ and $T'(t)$ according to their positivity or negativity.

3 Wind tunnel

The experimental flow is a spatially developping anisothermal mixing layer obtained in a specific low-speed mixing layer wind tunnel fed by two independent aeraulic circuits, both equipped with a 7.5 kW blower, a 42 kW cold battery and a 31 kW heater (figure 1). Two parallel streams

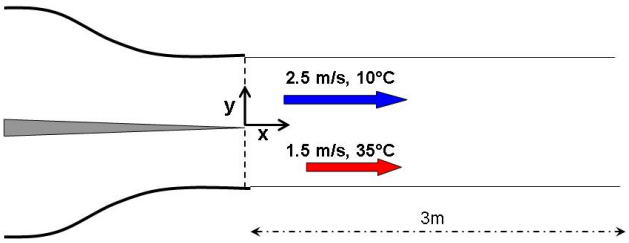

Figure 1. Diagrammatic representation of the low-speed wind tunnel (right) and flow configuration (left).

of different velocities and temperatures ([1.5 m/s, 2.5 m/s]; $[10°C, 35°C]$), are blown separately through two independent halves of a conditioning chamber comprising several screens and a slowly converging part (contration ratio: 2.25). The two streams are separated by a 52 mm thick thermal insulating plate.They then merge and initiate the mixing process downstream of the sharp end of a 1.5° tapered splitter plate made of aluminium. The mixing layer expands in a test section which is 3 m long and 1 m $\times$ 1 m in cross section. Downstream from the test section, the mixed flux is evacuated through a diverger.

At the entrance of the test section, the turbulence levels in the two parallel streams before mixing were lower than 1% for velocity and around 0.05°C for temperature. The thicknesses of the dynamic boundary layers measured at this location were $\Theta_{H.V.} = 2.15$ mm on the high velocity side and $\Theta_{L.V.} = 2$ mm on the low velocity side of the trailing edge of the splitter plate. The thickness of the thermal boundary layer was around 10 mm which is rather large due to the upstream thermal transfer through the sharp end of the splitter plate, but reasonably small for such experimental conditions.

4 Measurement system

A new hot wire anemometry technique was used to obtain simultaneous velocity and temperature measurements at the same location with a single wire (2.5 μm diameter, 0.5 mm long in the present study). The principle developed, named PCTA (Parameterizable Constant Temperature Anemometer), is based on the multiple overheat principle (Bruun (1995),Corrsin (1947)) and on specific signal processing. A detailed presentation of the PCTA principles in terms of electronic design, calibration, measurement, post-processing and uncertainty estimation can be found in Ndoye *et al.* (2010); Ndoye (2008). Only the main features of the method are recalled here.

4.1 PCTA principle

The PCTA principle is based on the implementation of a specific design allowing both rapid overheating and periodic variation in the overheat of the wire, making hence possible the reproduction of a unitary sequence of successive overheat levels at a constant frequency. The typical evolution of a triple overheat sequence is shown in figure 2. The number

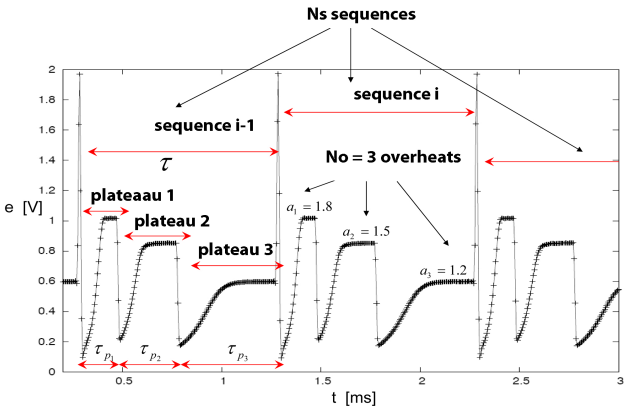

Figure 2. Typical time trace of PCTA output voltage, with multiple overheat sequencies of three overheat levels.

of overheat levels per sequence can vary from 2 to 8. The overheat duration can be set between 100 and 1000 μs to provide access to simultaneous high frequency velocity and temperature measurements at the same point. A minimization procedure allows the identification of instantaneous U and T decorrelated values from the data acquisition.The acquisition frequency can reach several kHz with a sufficiently thin wire. The performance of the PCTA is closely linked to the use of a dynamic calibration method in which the probe measures a periodically varying velocity associated with a decreasing temperature in a specific calibration wind tunnel.

4.2 Calibration and signal processing

The equation describing the relationship between a hot wire voltage response and the velocity temperature couple (U,T) in a anisothermal fluid flow can be chosen from various non-linear heat transfer equations, as described in particular by Bruun Bruun (1995). In the present study we used an

extended King's law:

$$e^2 = (a + bU^n)(T_w - T) \ , \qquad (1)$$

where e is the instantaneous voltage measured, and U and T are unknown. The wire temperature T_w, the coefficients a, b, and the exponent n are parameters associated with a given overheat level. For each overheat level of subscript k, within the overheat sequence of subscript i, the voltage measured is expressed as:

$$e_{i,k}^2 = (a_k + b_k U_i^{n_k})(T_{w,k} - T_i) \ . \qquad (2)$$

A single voltage value is automatically extracted for each overheat level assuming two important hypotheses: *i)* the repeatability of the overheat application is such that the parameters a, b, n and T_w are valid for a given overheat level on the whole set of sequences acquired, *ii)* U and T are considered constant on a given overheat sequence, which is equivalent to low pass filter U and T variations at the repetition frequency of the sequences. An optimization procedure, based on the Levenberg-Marquardt algorithms[1], is applied to extract the vectors of parameter $\mathbf{A_k} = \mathbf{a_k}, \mathbf{b_k}, \mathbf{n_k}, \mathbf{T_{w,k}}$ for each overheat level k, using calibration data. Another Levenberg-Marquardt procedure is applied to the instantaneous voltages in order to extract the velocity and temperature pairs (U_i, T_i) for each sequence integrated over the duration of the i^{th} multiple overheat sequence. The accuracy of the PCTA method was evaluated by estimating successively the uncertainty associated with the dynamic calibration, the measurement procedure and the post-processing technique, using a Monte Carlo simulation. For the PCTA operating in a three overheats configuration as shown in figure 2, and a calibration sample size of 3×10^5, the uncertainties are 1% for velocity and 0.15 K for temperature.

5 Results

The results on the flow characterization can be found in Ndoye (2008). The development distance of the flow (distance of appearance of the self-similarity of the fluctuations) was about $x/\Theta_{H.V.} = 500$. In the following figures showing transverse profiles across the mixing layer, the transverse coordinate y is replaced by the normalized coordinates, η_u for the velocity related curves and η_T for the temperature related curves. These normalized coordinates were defined in relation to the similarity references δ_ω and δ_T, which are the vorticity thickness and the thermal thickness of the mixing layer at the x location considered. The origins of these two normalized coordinates were positioned at the center of the dynamic and thermal mixing layers, respectively, the physical coordinates of which were $y_{0.5u}$ and $y_{0.5T}$, these two values being different as a result of the differences in the deflections of the mixing layers from the symmetry plane of the test section. The definition of the normalized coordinates are:

$$\eta_u = (y - y_{0.5u})/\delta_\omega \qquad \text{and} \qquad \eta_T = (y - y_{0.5T})/\delta_T \ . \qquad (3)$$

The subscripts HV,LT and LV,HT relate to the conditions applied on both sides of the mixing layer, ie High/Low Velocity and Temperature.

PDFs of velocity fluctuations were found to be nearly gaussian in the central region of the mixing layer and strongly asymmetric in the outer region on both sides. Temperature PDFs behaved in a non gaussian way with a peak the position of which varied across the layer in relation with the local mean value of the temperature.

Joint PDFs of $u'(t)$ and $T'(t)$ are shown in figure 3 for various transverse positions across the mixing layer width at a given streamwise location in the self similarity region. In the proximity of the edges of the mixing layer, the disymmetrical shape of the joint PDF shows the coexistence of blobs of low (respectively high) temperature, high (respectively low) velocity, barely mixed fluid (peak corresponding to small fluctuations), with a more turbulent flow part with isodensities close to gaussianity. The further we depart from the edges towards the mixing layer axis, the less the flow is influenced by the intermittencies. The fluid originating from both side of the mixing layer is then in a situation of turbulent mixing. Near the axis of the mixing layer, the isodensities are close to gaussianity (figure3-b). In a second stage, the mixing process was analysed with a quadrant splitting method (Lu & Willmarth (1973)) to provide a comprehensive study of the contributions to the heat flux from the principal fluid motions within the flow. The method consists in splitting the instantaneous heat flux $u'(t) \times T'(t)$ into four quadrants, each one being associated with one of the four possible combinations of the instantaneous values of the fluctuations $u'(t)$ and $T'(t)$ according to their positivity or negativity: I: $(u' > 0, T' > 0)$, II: $(u' < 0, T' > 0)$, III: $(u' < 0, T' < 0)$, and IV: $(u' > 0, T' < 0)$. The time-average of $u'(t) \times T'(t)$ in each quadrant was calculated, providing four conditionally averaged values of the heat flux at each measurement point.

These data were then used to quantify the contributions inside the turbulent thermal mixing process of the intermittencies associated with the saddle point ejections.

Figure 4 illustrates the classical mixing layer flow topology, and makes it possible to distinguish two types of macroscopic structures: large eddies and strands (fine zones that surround these eddies). At the center of the strand between two cores, lies a saddle point. Velocity and temperature fluctuation skewness presented in figure 5, shows that the predominant contribution to the fluctuation skewness (dominant intermittent events) are opposite for velocity fluctuations u' and temperature fluctuations T'. Furthermore, the saddle points are regions of significant fluid ejection out of the mixing layer. Each ejection produces an acceleration of the flow on the slow side and a deceleration on the rapid side, with vertical velocity fluctuations and longitudinal velocity fluctuations of opposite signs.

For example, in the present configuration, the rapid, cold uniform flow stream tends to strip off fluid intermittently from the saddle points. The mean temperature of this fluid originating from the cores is greater than that of the cold side, and its mean velocity is lower than the rapid velocity. Thus some hotter and slower fluids (leading to $T' > 0$ and $u' < 0$) are ejected from the saddle points towards the cold side, corresponding to quadrant II.

[1]The general principle of the Levenberg-Marquardt algorithms can be found in *Numerical Recipes in Fortran* Press *et al.* (1992)

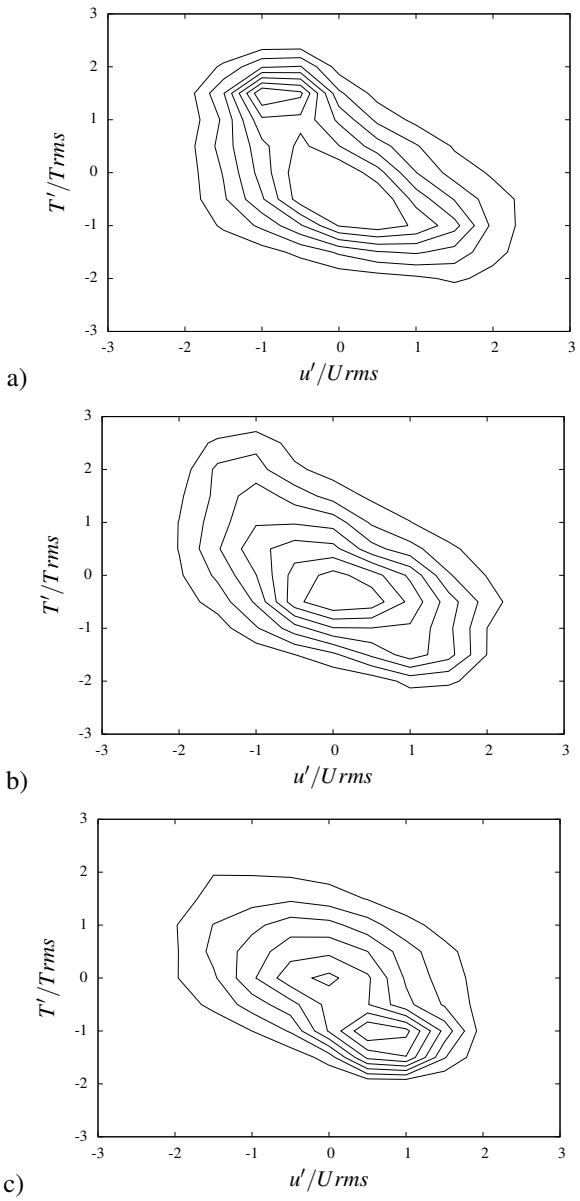

Figure 3. Variations in the temperature joint PDF across the mixing layer: a) near the slow and hot side edge ($y/\delta_\omega = -0.3$); b) near the mixing layer axis ($y = 0$); c) near the rapid and cold side edge ($y/\delta_\omega = +0.3$).

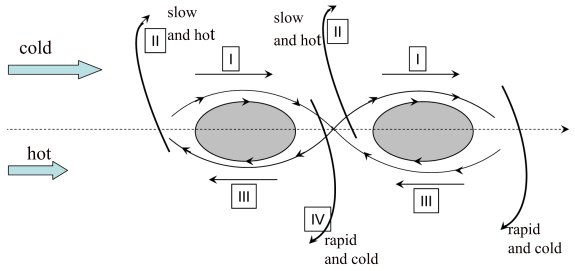

Figure 4. Diagrammatic representation of the principal fluid movements contributing to the heat flux in an anisothermal mixing layer.

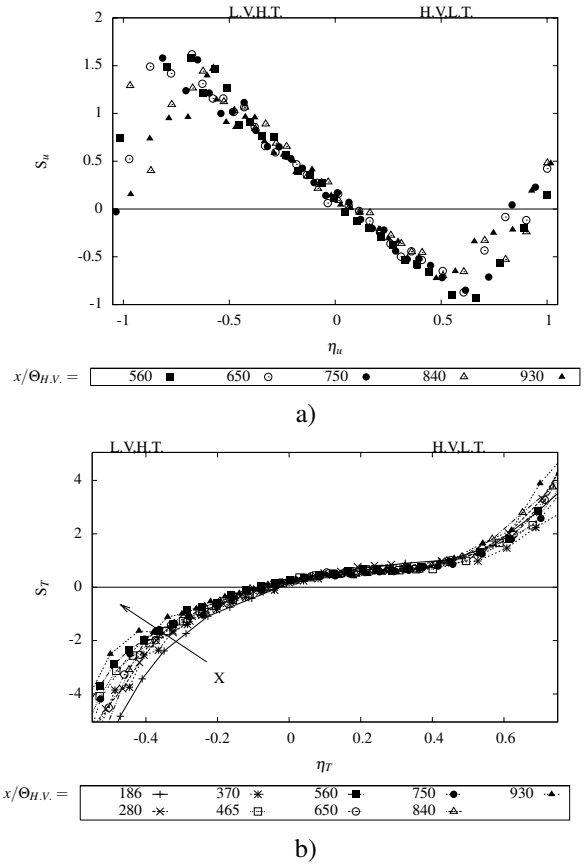

Figure 5. Skewness factor: (a) velocity, (b) temperature.

Similarly, the region of uniform hot, slow flow strips off some cold fluid from the saddle points. The fluid originating from such ejections is colder and faster than the uniform part of the flow on that side, corresponding to quadrant IV. From similar analysis it appears that quadrants I and III correspond to interactions between the pheriphery of the structures and the outer regions of uniform flow.

When analyzing the joint PDF through the $u'T'$ quadrant approach (figure 6), the main part of the heat flux appears dominated by quadrants II and IV which were identified as associated to the saddle point ejections either of slow and hot fluid (II) or rapid and cold fluid (IV). This trend was confirmed by the comparison of the quadrants relative contributions to the longitudinal heat flux as reported in figure 6 for different x positions. Each graph shows the transverse profiles of $\overline{u'(t) \times T'(t)}$ separated into four curves, each one corresponding to a quadrant. The magnitude of $\overline{u'(t) \times T'(t)}$ is representative of the respective strengths of the four contributions to the heat flux. Downstream from the wake region, the contributions of I and III evolve towards profiles shifted on opposite sides of an axis of symmetry located on the axis of the dynamic mixing region ($y_{0.5u}$). The interactions between the peripheries of the coherent structures and the uniform parts of the flow thus appear nearly symmetrical in relation to the dynamic mixing layer axis. They reach a maximum

value at the mixing layer edges, and decrease towards a zero value in the uniform flow region. This corresponds well to the topology of figure 4 where quadrants *I* and *III* are associated with the cores of the structures in the dynamic mixing zone. In parallel, the magnitude of the contributions of quadrants *II* and *IV* becomes greater, reflecting a predominance, within heat flux, of the fluid ejections, which behave symmetrically in relation to the thermal mixing region axis (located at $y_{0.5T}$). This growing contribution of quadrants *II* and *IV* corresponds to the shape of the joint PDFs seen in figure 3, where the fluctuations T' associated to the opposite sign of u' are dominant in the self similarity region.

In the self-similarity region, the dominating movements appear to be ejections. The intensity of the interactions between the periphery of the structures and the outer zones of the uniform flow decreases gradually with x while the intensity of the ejections increases. The quadrant analysis can then clearly highlight the fact that the expansion of the dynamic and thermal mixing layers is associated with a growing domination of saddle point ejections and a weakening interaction between the structures and the outer regions of the mixing layer.

6 Conclusion

The correlations between velocity and temperature fluctuations were investigated across the mixing layer using the ability of the variable temperature hot wire anemometer to deliver simultaneous measurements of velocity and temperature at the same point. Showing a progressive drift from gaussianity as they move toward the edge of the mixing layer, the velocity temperature joint PDF patterns were analyzed by means of a quadrant analysis in which the heat flux was split into four components according to the positivity or negativity of $u'(t) \times T'(t)$. This study showed the ability of the variable temperature hot wire anemometry to deliver consistent velocity and temperature instantaneous values at the same point allowing the analysis of the contribution of the saddle point ejections in the mixing process.

REFERENCES

Batt, R. G. 1977 Turbulent mixing of passive and chemically reacting species in a low speed shear layer. *J. Fluid Mech.* **82**, 53–95.

Bisset, D. K. 1997 Numerical simulation of heat transfer in turbulent mixing layers. In *Proceedings of 13th Australasian Fluid Mechanics Conference*, pp. 21–24.

Brown, G.L. & Roshko, A. 1974 On density effects and large structure in the turbulent mixing layers. *J. Fluid Mech.* **64**, 775–816.

Bruun, H. H. 1995 Hot-wire anemometry: Principles and signal analysis. *Tech. Rep.*. Oxford University press Inc., New York, USA.

Corrsin, S. 1947 Extended application of the hot wire anemometer. *Rev. Sci. Inst.* pp. 469–471.

Fiedler, H. E. 1974 Transport of heat across a plane turbulent mixing layer. *Advances in Geophysics* **18 A**, 93–109.

Karasso, P. S. & Mungal, M. G. 1996 Scalar mixing and reaction in plane liquid shear layers. *J. Fluid Mech.* **323**, 23–63.

Lu, S. S. & Willmarth, W. W. 1973 Measurements of the structure of the Reynolds stress in a turbulent boundary layer. *J Fluid Mech.* **60**, 481–511.

Masutani, S. M. & Bowman, C.T. 1986 The structure of a chemically reacting plane mixing layer. *J. Fluid Mech.* **172**, 93–126.

Ndoye, M. 2008 Anémométrie fil chaud: application l'étude d'une couche de mlange anisotherme. PhD thesis, Université de Poitiers, France.

Ndoye, M., Delville, J., Heitz, D. & Arroyo, G. 2010 Parameterizable constant temperature anemometer: a new method for the analysis. *Meas. Sci. Technol.* **21 (7)**.

Perry, A. 1982 Hot-wire anemometry. *Tech. Rep.*. Clanderson Press, Oxford, UK.

Pickett, L. M. & Ghandi, J. B. 2001 Passive scalar measurements in a planar mixing layer by PLIF of acetone. *Exp. Fluids* **31**, 309–318.

Pickett, L. M. & Ghandi, J. B. 2002 Passive scalar mixing in a planar shear layer with laminar and turbulent inlet conditions. *Phys. Fluids* **14**, 985–998.

Press, W. H., Teutolsky, S. A., Vetterling, W. T. & Flannery, B. P. 1992 The art of scientific computing - second edition. numerical recipes in fortran. *Tech. Rep.*. Cambridge University Press.

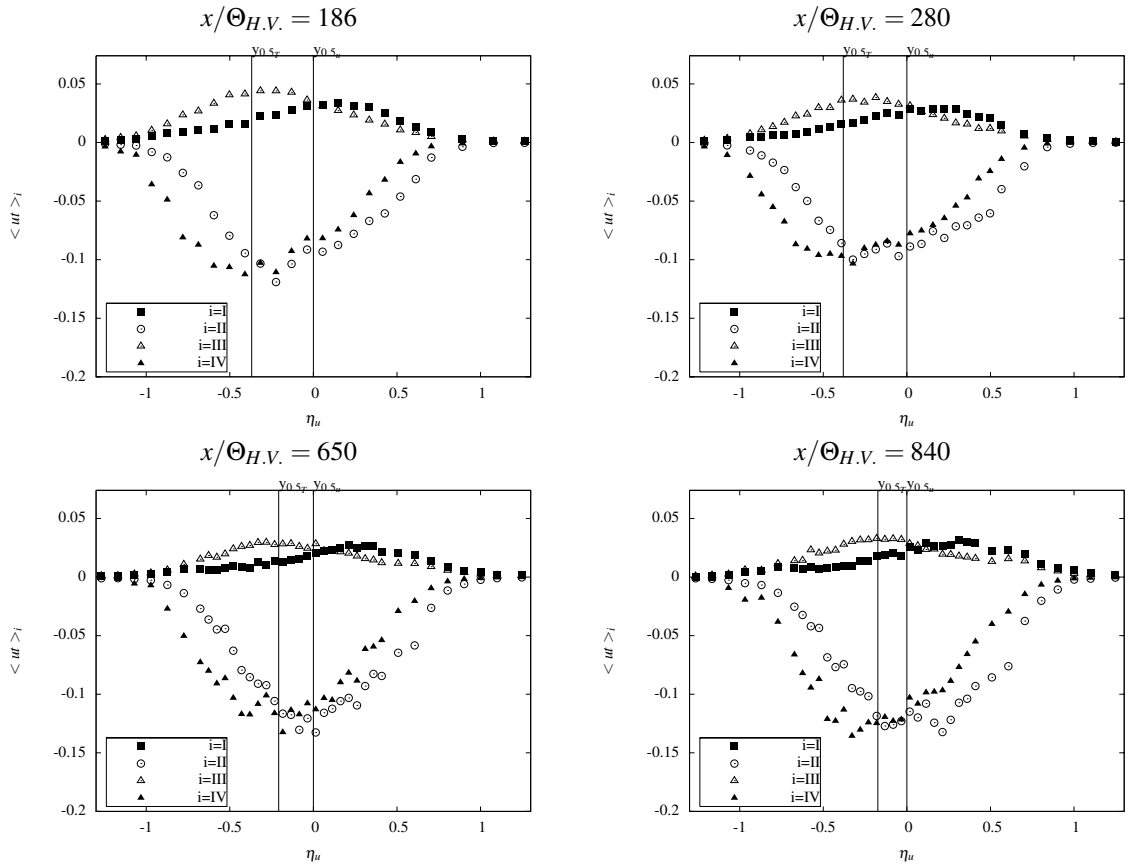

Figure 6. Quadrant heat flux contribution: transverse profiles of the averaged value of $u'(t) \times T'(t)$ splitted into four quadrants.